Peptide Models of Folding Initiation Sites of Bovine β-Lactoglobulin: Identification of Nativelike Hydrophobic Interactions Involving G and H Strands†

Laura Ragona,‡ Maddalena Catalano,‡ Lucia Zetta,‡ Renato Longhi,§ Federico Fogolari,|| and Henriette Molinari*,‡,||

Laboratorio NMR, ICM, via Ampère 56, 20131, Milano, Italy, Istituto di Biocatalisi e Riconoscimento Molecolare, CNR, via M. Bianco, 20131 Milano, Italy, and Dipartimento Scientifico e Tecnologico, Università degli Studi di Verona, Strada Le Grazie 15, 37134 Verona, Italy

Received August 6, 2001; Revised Manuscript Received January 2, 2002

ABSTRACT: In an attempt to characterize the early folding events in bovine β-lactoglobulin (BLG), a set of peptides, covering the flexible N-terminal region and the stable C-terminus β-core, was synthesized and analyzed by circular dichroism and by nuclear magnetic resonance in water, trifluoroethanol (TFE), and sodium dodecyl sulfate (SDS) below and above the critical micellar concentration. The role of local and long-range hydrophobic interactions in guiding the folding has been investigated. For the peptide fragment covering the more flexible N-terminal region of BLG (β-strands A, B), where both theoretical predictions and kinetic refolding experiments suggested the formation of non-native α-helix, no native long-range contacts were identified, and a helical secondary structure was stabilized only in the presence of 25 mM SDS. At variance, in 50% (v/v) TFE, native, long-range hydrophobic interactions were observed in the peptide covering the core region comprising G and H β-strands. The side chains involved in these interactions form a nativelike hydrophobic cluster, thus suggesting that the GH region may act as the folding initiation site for BLG. This result is reinforced by the identification, in the urea denaturated BLG, of residual structure located at the level of the GH interface, as evidenced by NMR analysis. These results, in excellent agreement with kinetic, thermodynamic, and cold denaturation folding data, once more underline the utmost importance of the GH region for the stability and folding of BLG. Severe aggregation effects prevented the structural analysis of the peptide covering the EFGH region, indicating that this larger segment does not represent an independent folding domain and that the terminal α-helix is necessary for stabilizing the BLG folding core.

The structural and folding properties of bovine β-lactoglobulin (BLG),[1] the major whey protein abundant in cow's milk, have been reported by us and others (*1*−*8*) and have evidenced some very interesting features. Although BLG displays a β-barrel structure, it has a markedly high helical propensity (*1*, *9*). It was first proposed, on the basis of CD and SAXS experiments, that an intermediate with nonnative α-helical structure is accumulated during refolding, suggesting that local interactions between neighboring amino acid residues may play a major role in favoring the formation of α-helical structures (*10*).

Hydrogen exchange measurements performed at different urea concentrations (*6*) indicated the presence of a unique cooperative unfolding unit, encompassing all the eight β-strands (A−H), except strand I, and the terminal region of the terminal α-helix. We have shown that the slowest exchanging amides joining a common isotherm at 2 M urea can be divided in two classes: (i) those localized within E, F, G, H strands, showing a linear dependence of the free energy of opening from urea concentration, thus exchanging through a global unfolding mechanism; and (ii) those mainly localized in the N terminal region of the protein, at the level of A, B, C and D strands, showing local structural fluctuations at very low urea concentration.

Refolding H/D pulse labeling experiments (*8*) indicated the presence in the native state of a stable hydrophobic core consisting of F, G, and H strands. Moreover, it was recently observed, using ultrarapid mixing techniques in conjunction with fluorescence detection and hydrogen exchange labeling probed by heteronuclear NMR, that, within 2 ms of refolding, well protected amide protons, indicative of stable hydrogen bonded structures, were found only in a domain comprising strands F, G, H, and the terminal helix (*11*). In addition, a marginally stable transient nonnative α-helical structure was localized near the N-terminus end (residues 12−21), although its role in determining the pathway and rate of folding needs to be clarified.

In this respect BLG represents an intriguing model for studying the interplay between local and nonlocal interactions in guiding the folding.

To further investigate earlier events in folding, we took the approach of studying peptide fragments corresponding

† This work was supported by the Italian National Council of Research "Comitato Biotecnologie" and by the Italian Ministry of University and Scientific Research (MURST). M. Catalano is a fellow of the "Fondazione Antonio De Marco".

* To whom correspondence should be addressed. Phone: 00 39 027 064 3554. Fax: 00 39 027 064 3557. E-mail: Henry@icmnmr.mi.cnr.it

‡ Laboratorio NMR.

§ Istituto di Biocatalisi e Riconoscimento Molecolare.

|| Dipartimento Scientifico e Tecnologico.

[1] Abbreviations: CD, circular dichroism; cmc, critical micellar concentration; NMR, nuclear magnetic resonance; SDS, sodium dodecyl sulfate; TFE, 2,2,2-trifluoroethanol.

10.1021/bi011615r CCC: $22.00
Published on Web 01/26/2002

to selected regions of BLG secondary structure. This approach, well documented in the literature (*12*−*14*), has been used quite often to detect both stable and nascent secondary structures and/or hydrophobic clusters which can be of primary importance in determining the folding pathway of a protein.

In this work, we report CD, NMR, and molecular dynamics structural studies of fragment peptides reproducing selected regions of BLG covering both the flexible N-terminus and the stable β-core folding domain.

Peptides corresponding to BLG single strands A, D, F, and to the terminal helix were previously synthesized and studied by CD and NMR in the presence of 50% (v/v) TFE (*15*, *16*), revealing the presence of helical structures. We decided instead to synthesize peptide fragments long enough to cover two contiguous β-strands of BLG in order to allow for the formation of long-range interactions. The criteria followed to select protein regions to be studied were based on the results of H/D exchange experiments performed on the intact protein (*6*, *8*). Indeed it was clear that most of the residues showing both high α-helical propensity, as determined by structural propensity predictions (*1*, *9*) and conformational fluctuations in the native state, were located mainly in the N-terminal part of the protein, where nonnative α-helices were suggested to be formed, while the stable and rigid hydrophobic core was localized at the levels of strands F, G, and H.

Structural results obtained for the peptide fragments in water and in the presence of variable amounts of cosolvents, such as TFE and SDS, are compared with the corresponding structured regions of the native BLG in order to draw conclusions about the early folding steps.

MATERIAL AND METHODS

Peptide Synthesis. The peptides were synthesized by solid-phase methods on an automated Applied Biosystem model 433A peptide synthesizer using N^a-[9-fluorenyl(methoxy-carbonyl)] (FMOC)-protected amino acids and 2-(1H-benzo-triazol-1-yl)-1,1,3,3-tetramethyluronium tetrafluoroborate (HBTU) or O-(7-azabenzotriazol-1-yl)-1,1,3,3-tetramethyl-uronium hexafluorophosphate activation chemistry. The peptide chain was assembled stepwise on 2-chlorotrityl resin (*17*) and derivatized with the appropriate amino acid (0.4 mequiv/g). Cleavage from the resin was performed with mixture K including 2% triisopropylsilane (*18*).

The peptides were purified to homogeneity of >96% using semipreparative reversed-phase high-performance liquid chromatography (RP-HPLC) on a Vydac C4 column (10 × 250 mm) using an acetonitrile/water gradient, and the peptides were recovered in 40−60% yield. The peptide EFGH which contains two cysteines, was oxidatively folded by overnight treatment with 5-fold excess of oxidized glutathione; the peptide concentration was 0.05 mM, in 25% (v/v) TFE, 20 mM Tris-buffer, pH 8 (*19*). Progress of peptide folding was monitored by analytical HPLC on a Vydac C4 column; finally the peptide was purified from polymeric material by semipreparative RP-HPLC.

Purity was verified by analytical RP-HPLC, on a Whatman C-18 or on Vydac C4 column, using a linear gradient of acetonitrile in water containing 0.1% trifluoro-acetic acid. The amino acid composition was confirmed by quantitative amino acid analysis; the mass of the peptides was measured by matrix-assisted laser desorpion/ionization time-of-flight mass spectrometry on a Voyager-RP Biospectrometry Workstation (PerSeptive Biosystem Inc.).

Circular Dichroism Analysis. CD spectra were collected using a Jasco J500 spectropolarimeter. Spectra were run at 37 °C at polypeptide concentration of 50 μM with a cuvette path length of 0.1 cm. All spectra were baseline corrected by subtracting buffer spectra. The molar ellipticity was calculated according to

$$[\Theta]_\lambda = \frac{\Theta_\lambda \times 100}{[(N-1)lc]} \quad (1)$$

where Θ_λ is the measured ellipticity (in degrees) at a wavelength λ, N is the number of residues, l is the cuvette path length (in cm), and c is the protein concentration (in mol/L). The helical population of the peptides in the different solution conditions was estimated from the measured mean-residue ellipticity at 222 nm ($[\theta]_{222}$). Using the following equation,

$$\%\ \text{Helix} = \frac{([\Theta]_{222}^{\text{obs}} \cdot 100)}{([\Theta]_{222}^{\text{helix}})} \cdot \left[1 - \frac{2.57}{(N-1)}\right] \quad (2)$$

where $[\Theta]_{222}^{\text{helix}}$ is the ellipticity of a peptide of infinite length with 100% helix population, taken as $-39\,500$ deg^2 dmol^{-1} at 222 nm and N is the number of residues (*20*).

The effect of peptide concentration on far-UV CD spectra in 50% (v/v) TFE was determined by acquiring three spectra at peptide concentrations of 25 μM, 250 μM, and 1.2 mM in 0.025 mm, 0.1 mm, and 1 mm cuvettes, respectively. The recorded spectra showed no dependence from peptide concentrations.

^{1}H NMR Spectroscopy. All NMR spectra were acquired on a Bruker DMX 500 MHz spectrometer. Data acquisition for the homonuclear TOCSY (*21*) and NOESY (*22*) spectra were carried out in a temperature range of 17−37 °C. The size of the acquisition data matrix was 2048 × 512 data points in f_2 and f_1, respectively, and a sweep width of 5500 Hz in both dimensions was used. Water suppression was achieved by low power irradiation during the relaxation delay introduced between scans or by 3-9-19 pulse sequence with gradients (*22*). For TOCSY spectra various isotropic mixing times were employed, ranging from 20 to 90 ms, while for NOESY experiments, mixing times of 100, 150, 200, and 250 ms were employed.

Peptide concentrations were typically 1.2 mM in all tested solvents. Spectra were recorded in aqueous phosphate buffer (H_3PO_4/NaOH 10 mM) at pH 2.1 and at different TFE concentrations (10%, 20%, 30%, 50% v/v). The final 50% (v/v) TFE solution, for structure determination, was chosen to maintain the conditions reported in the literature for the structural studies of shorter BLG peptides (*1*). NMR spectra were also recorded in sodium dodecyl sulfate (SDS) below and over the critical micellar concentration (cmc = 8 mM).

EFGH showed extensive aggregation in water. Other solution conditions were tested [50% (v/v) TFE and 2 mM SDS] without any improvement of the quality of NMR spectra.

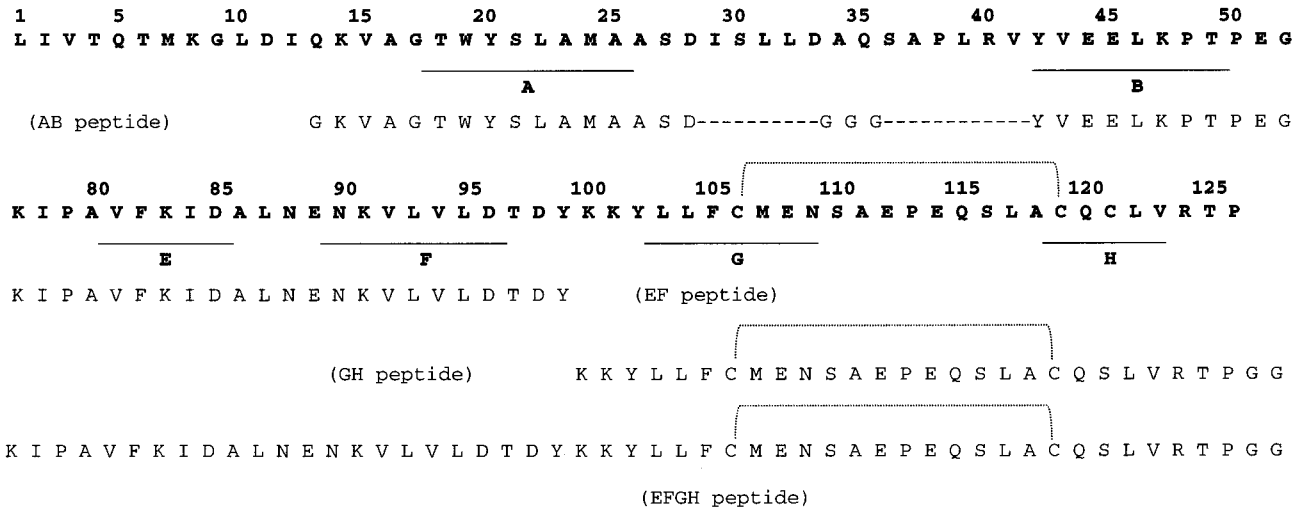

FIGURE 1: Amino acid sequences of the N-terminus (1−52) and of the stable core region (77−126) of BLG (in bold) and of the synthesized peptides AB, EF, GH, and EFGH. Continuous lines represent the β-strand regions while dotted lines the disulfide bridges.

NMR assignments were made using a combination of TOCSY, DQF-COSY, and NOESY spectra using the program XEASY (*23*). The assignment of NOESY spectra was checked with the program NOAH, combining an automated assignment with structural calculations (*24*). The list of proton chemical shifts for AB peptide in 50% (v/v) TFE and 25 mM SDS and for GH peptide in water, 50% (v/v) TFE, and 2 mM SDS are available as Supporting Information. Chemical shift referencing for all the acquired spectra was obtained using TSP dissolved in the sample solutions.

For the analysis of BLG residual structure, different samples containing the same amount of protein (1 mM) were prepared in deuterated phosphate buffer solutions at pH 2.1 with different quantities of urea (in the range 0−7 M). Both 1D and 2D TOCSY (mixing time 50 ms) and NOESY (mixing time 100 ms) experiments were recorded and analyzed as described before for peptides.

Conformational Shifts. Conformational shift maps were obtained using as reference the random coil chemical shifts reported by Wishart (*25*). Although these reference shifts were obtained in water at pH 5 and 25 °C, they were reported to be insensitive to the solution conditions, as very small deviations (±0.02 ppm) were observed when several random coil chemical shifts were measured in 30% (v/v) TFE, at pH 5.4 and 22 °C (*26*). To calculate average conformational shifts toward α-helix, only upfield shifts in the regions of the peptides assumed to be helical were considered. A zero contribution was assigned to the small upfield shifts occurring at the termini. For glycine residues, lacking stereospecific assignments, we used the larger upfield shift to compute the average. The average conformational shift was calculated by adding all upfield shifts and dividing by the total number of peptide bonds. To obtain overall helical contents for each peptide, the average conformational shifts were divided by 0.35 ppm, which was assigned as an average for 100% helicity, as reported in ref *27*.

Structure Calculations. Calculated structures were obtained from restrained molecular dynamics simulations using DYANA (*28*) followed by energy minimization using the AMBER force-field as implemented by the program DISCOVER (Molecular Simulations, San Diego, CA). Volume integration was performed on NOESY spectra with mixing times of 150 ms for AB peptide in 25 mM SDS and 200 ms for GH peptide in 50% (v/v) TFE. The list of distance restraints obtained from NOAH program, accurately checked on NOESY spectra, was used as input for DYANA calculations. For GH peptide, NOE restraints were supplemented by six distance restraints for the disulfide bridge formed between C7 and C20. ϕ angle restraints were derived from $^3J_{N\alpha}$ constants estimated by the separation of extrema in dispersive and absorptive plots of rows through DQF-COSY cross-peaks (*29*).

One hundred calculations with the program DYANA were started with random polypeptide conformations and the 20 resulting conformers with the lowest residual target function values were analyzed. The restraints were reexamined in view of consistent violations and relaxed where necessary. This procedure was repeated until no consistent violations were found in half or more of the structures. After this step, 100 new DYANA calculations were started, and the 20 structures with the lowest target functions were further refined using the AMBER force field. Each structure was minimized performing 100 steps of steepest descent and 300 steps of conjugate gradient. The 10 structures with the lowest potential energy were selected for further analysis. RMSD values for all the peptides were calculated over the range of residues showing medium distance restraints (i.e., between amino acids at positions i and j, with $i - j \geq 2$).

RESULTS

We have synthesized the following fragments (Figure 1): (i) peptide AB, covering BLG residues 14−28 (A strand) and 42−52 (B strand), where the long, flexible and exposed AB loop was substituted with a GGG linker (*30*); (ii) peptide GH, covering the BLG region 100−126; (iii) peptide EF, covering the region 77−99; and (iv) peptide EFGH covering the 77−126 region.

Circular Dichroism. The CD spectra of the studied peptides in different solution conditions are reported in Figure 2. Peptide EF could not be considered in our analysis due to its very low solubility. It showed the tendency to form high molecular weight aggregates which prevented further structural characterization. The CD spectra of the other peptides indicated that they are largely unstructured in water at 37

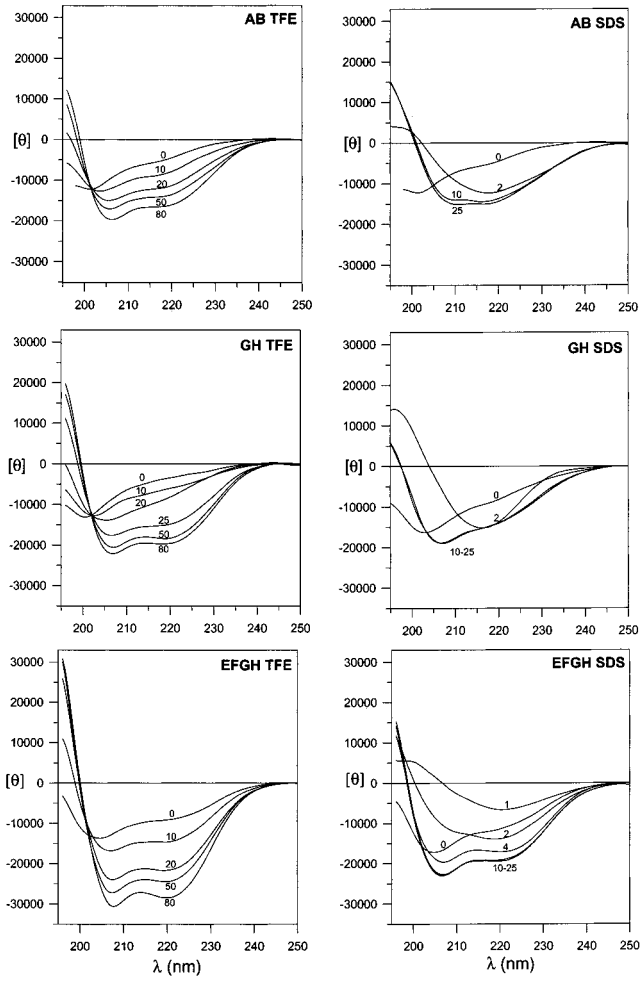

FIGURE 2: Far-UV CD spectra of AB, GH, and EFGH peptides recorded at 27 °C in various solvent conditions. The name of the peptide and the employed solvent are reported in the upper right corner of each graph. Numbers indicate the concentration of TFE in % (v/v) and the molar concentration of SDS, respectively.

°C. Upon addition of TFE (in the range 10−80%), the peptides showed a shift in the minimum toward 208 and 222 nm. The strong helical tendency of EFGH peptide in TFE parallels the behavior reported for BLG in 50% (v/v) TFE (*3*, *30*). It is interesting to observe that when SDS below the critical micellar concentration was used as a cosolvent, all peptides showed CD spectra somehow reminiscent of β structures, while pattern characteristics of α-helices were apparent in 25 mM SDS. It has been shown that in the presence of a low concentration of SDS (2−4 mM) and depending on molar ratio of SDS to peptide, equivocal sequences may assume β structures (*31*). Wu and co-workers (*32*) found that even if nonmicellar SDS has the tendency to promote β structures, peptides without any structure-forming potential remained disordered regardless of surfactant concentration. Hence β structure formation is not a common property in short peptides in SDS below the cmc, as confirmed by many examples reported in the literature (*14*).

It is interesting to note that the observed helicity of the AB peptide in 50% (v/v) TFE (ca. 29%) is roughly one-half the value obtained (ca. 63%) for the previously studied peptide corresponding to the single A strand (*1*).

NMR Spectroscopy and Molecular Dynamics Simulations. (i) Peptide AB. This peptide was characterized by NMR in aqueous phosphate buffer at pH 2.1, in 50% (v/v) TFE, and in 25 mM SDS in the temperature range 17−27 °C. It is worth noting that peptide covering strand A alone could not be studied by NMR since it formed gels both in water and in 50% (v/v) TFE at 1 mM concentration.

Peptide AB showed a poor dispersion in water and, due to severe overlap, only few spin systems could be assigned. In 50% (v/v), TFE solution multiple conformations were detected in the 20−24 region, and only three $\alpha\beta(i,i+3)$ NOEs were detected in the segment 7−14, showing few H^{α} secondary shifts higher than 0.3 ppm (Figure 3). The number of unambiguous NOE contacts was not sufficient (<6 NOEs/residue) to perform a reliable structure calculation. Due to extensive aggregation at high concentration, peptide AB could not be analyzed by NMR in the presence of 2 mM SDS. When the SDS concentration was raised above the cmc, the α-helical content increased, with an apparent stabilization of the C-terminal region of the peptide. The detection by NMR of the presence and extension of a helical conformation was based on the following observations: (i) a stretch of nonsequential $\alpha N(i,i+3)$, $\alpha N(i,i+4)$, $\alpha\beta(i,i+3)$ NOE connectivities; (ii) strong or medium sequential NN NOE connectivities together with medium sequential αN NOEs; (iii) significant upfield shifting (>0.3 ppm) of H^{α} resonances; (iv) $^3J_{\alpha N}$ coupling constants lower than 5 Hz. As summarized in Figure 3, NOEs typical of helical conformations could be unambiguously detected only in the C-terminal region of the peptide. One hundred calculations with the program DYANA were started with random polypeptide conformations and the obtained 10 best structures exhibited RMSD values, calculated for the backbone and all heavy atoms, in the region 2−25, of 5.37 ± 0.75 Å and 6.50 ± 0.81 Å, respectively (see Table 1).

(ii) Peptide GH. Despite the CD data showing that GH peptide did not show any conformational preference in water, we performed an NMR characterization of the peptide in aqueous solution. It should be noted that multiple conformations, indicated by the presence of additional cross-peaks of minor intensity, were present. The H^{α} secondary shifts showed essentially random conformation. The NOE data were not sufficient to perform a structure calculation; however, it is worth noting that the careful analysis of the NOESY spectra revealed the presence of a weak long-range cross-peak that could be assigned to the dipolar correlation between $H_{3,5}$ of F6 (*F105*, BLG numbering) and $H_{\delta/\delta'}$ of L23 (*L122*) (see later). This cross-peak could be identified because L23 (*L122*) is the only leucine residue exhibiting one of the two δ-methyl resonances at lower field (0.87 ppm) with respect to all the other leucines (showing one of the two δ-methyl groups at 0.84 ppm) (see Supporting Information).

The GH peptide could be carefully analyzed in 50% (v/v) TFE, and Figure 4 reports all relevant NOE data and H^{α} secondary shifts. Interestingly TFE did not seem to induce any well-defined helical structure, as judged on the basis of the criteria indicated above for the presence and extension of helical conformations. At least nine coupling constants higher than 7.5 Hz, typical of extended structures, were detected. The presence of a kink in the structure, related to the disulfide bridge between C7 and C20, was suggested by the observation of an inversion of the H^{α} secondary shifts in the region 12−13, culminating with a positive value higher than 0.5 ppm for residue E13. A few unambiguous long-

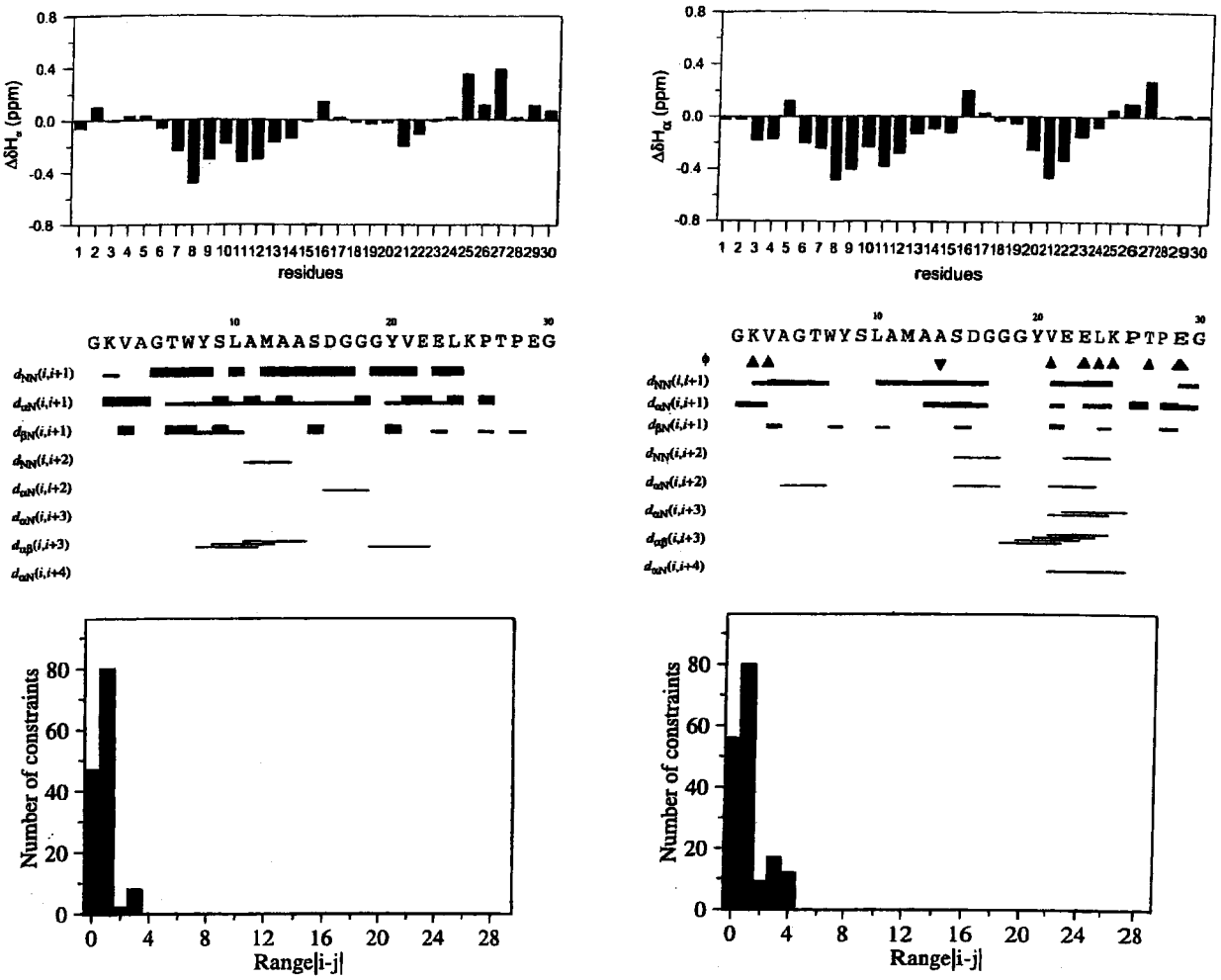

FIGURE 3: AB peptide in 50% (v/v) TFE (left panels) and in 25 mM SDS (right panels) at 17 °C. The conformational H_α $\Delta\delta$ shifts ($\Delta\delta = \delta^{obs} - \delta^{RC}$), where δ^{RC} are the shifts corresponding to random coil values (*25*), are diagrammatically represented (top panels) as a function of sequence number. Sequence and summary of NOE connectivities observed in solution (middle panels); the thickness of the lines reflects the intensity of the sequential NOE connectivities, i.e., weak, medium, and strong. In the right middle panel, ϕ values typical of helical structures are indicated (▲) (measured coupling constants $^3J_{\alpha N} < 5$ Hz), while ϕ values typical of extended structures are indicated (▼) (measured coupling constants $^3J_{\alpha N} > 7.5$ Hz). Number of restraints used for structure calculation versus the distance in the primary sequence among the interacting residues (bottom panels).

range NOEs were detected (Figure 4, Table 2) which were responsible for the conformational preference observed in the structures obtained after molecular dynamics simulations performed with the program DYANA and the minimization procedure, as described in Materials and Methods. The superposition of the 10 energy-minimized DYANA conformers, reported in Figure 5, afforded RMSD values, calculated for the backbone and all heavy atoms in the region 3−25, of 2.97 ± 1.20 Å and 3.84 ± 1.25 Å, respectively. Table 1 reports all the parameters characterizing the energy minimized NMR structures of the peptide.

The results of the structure determination show that the polypeptide backbone of residues at the N and C-termini are close and that the orientations of few hydrophobic side chains are well defined and form a native hydrophobic cluster (see later). The notion that the observed structural preference represents a meaningful structure determination and it is not only due to the presence of the native disulfide bridge C7−C20 (*C106−C119* in BLG numbering), which was maintained in the synthesized peptide, is supported by comparison with a corresponding group of 20 DYANA conformers, calculated without experimental restraints, except for those due to the disulfide bridge. These conformers display larger RMSD values [$RMSD_{bb}(3-25) = 5.27 \pm 1.19$ Å and $RMSD_{heavy}(3-25) = 6.90 \pm 1.08$ Å to be compared with $RMSD_{bb}(3-25) = 3.34 \pm 1.07$ Å, $RMSD_{heavy}(3-25) = 4.47 \pm 1.14$ Å] for the restrained structure calculations and do not show any native hydrophobic cluster (see later).

To extend the comparison of the peptide structural preferences to observations in the same solvent, we dissolved the GH peptide both in 2 mM and in 25 mM SDS. The opposite behavior with respect to peptide AB was observed: indeed it was possible to assign the spectrum in 2 mM SDS, while at SDS concentration higher than cmc, extensive aggregation prevented the NMR assignment. The peptide exhibited H^α secondary shifts typical of random coil (see later) and no further analysis was performed.

(iii) Peptide EFGH. This peptide was highly aggregated in phosphate buffer solution at pH 2.1, as clearly shown by its fingerprint region reported in Figure 6. A tentative assignment was only possible for the four aromatic residues and for residues L46, V47, R48, starting from the spin system of the unique arginine residue. Most of the methyl moieties resonate at 0.9 ppm, typical of random coil, even if few methyl groups were upfield shifted at 0.6−0.7 ppm. The spectra did not improve upon addition of TFE and SDS and

Table 1: Conformational Restraints and Structural Parameters of Molecular Dynamics Simulations

	AB in 25 mM SDS	GH in 50% (v/v) TFE
(a) restraints		
no. of upper distance restraints	174	222
no. of torsion angle (ϕ) restraints	9	12
(b) DYANA	20 structures	20 structures
target function (Å^2)	$6.65 \pm 2.56 \times 10^{-2}$	0.51 ± 0.11
avg no. of upper restraints violations > 0.25 Å/structure	0	1.5
maximum violation (Å)	0	0.52
avg no. of angle restraints violations > 5°/structure	0	0
maximum violation (degree)	0	0
$<RMSD_{bb}>$ (Å)[a]	5.02 ± 0.88	3.34 ± 1.07
$<RMSD_{heavy}>$ (Å)[a]	6.34 ± 0.97	4.47 ± 1.14
(c) Discover (AMBER force field)	10 best structures	10 best structures
total energy (kcal/mol)	-51.4 ± 5.6	-38.6 ± 4.5
bond energy energy (kcal/mol)	3.6 ± 0.2	4.2 ± 0.2
angle energy (kcal/mol)	25.3 ± 1.2	37.7 ± 3.5
torsion energy (kcal/mol)	21.7 ± 2.7	32.2 ± 1.9
out of plane energy (kcal/mol)	0.6 ± 0.1	0.9 ± 0.2
hydrogen bond energy (kcal/mol)	-6.3 ± 1.0	-6.7 ± 0.7
Lennard-Jones energy (kcal/mol)	-42.5 ± 5.0	-66.3 ± 4.7
Coulomb energy (kcal/mol)	-56.7 ± 3.1	-49.3 ± 1.5
restraining potential energy (kcal/mol)	3.0 ± 1.0	8.7 ± 1.5
avg no. of upper restraints violations > 0.25 Å/structure	0.4	2.6
maximum violation (Å)	0.31	0.5
avg no. of angle restraints violations > 5°/structure	0	0.1
maximum violation (degree)	0	5.4
$<RMSD_{bb}>$ (Å)[a]	5.37 ± 0.75	2.97 ± 1.20
$<RMSD_{heavy}>$ (Å)[a]	6.50 ± 0.81	3.84 ± 1.25

[a] RMSD values were calculated over a residue range of 2−25 and 3−25 for AB peptide in 25 mM SDS and GH peptide in 50% (v/v) TFE, respectively.

no further structural characterization could be performed on this peptide.

Comparison between Far-UV CD and NMR Helix Populations. It is well established that quantitative information about helical population of short peptides may be extracted from the analysis of the conformational shifts of H^α protons (*27*, *33*, *34*). In fact while a detailed comparison of the helicity at the residue level using NOEs is hampered by cross-peak overlap problems and by quantitation difficulties, chemical shifts can be measured accurately and are not affected by the existence of different correlation times. The helix population of AB and GH peptides in 50% (v/v) TFE, calculated using the NMR information, is 26% for both peptides, to be compared with 29% and 40%, respectively, obtained from CD data. A good correlation is observed for the results of the two methods relative to AB peptide in 50% (v/v) TFE solution. Helix population appears to be overestimated by CD for GH peptide in 50% (v/v) TFE, as expected due to the contribution of the disulfide bridge in the far UV region (*35*). The figures obtained by CD and NMR in SDS solutions could not be directly compared due to the different SDS to peptide molar ratio used for CD and NMR experiments. In fact, as a consequence of the different concentrations required by the two techniques, a 30-fold increase in the SDS to peptide molar ratio was employed in CD measurements.

For GH peptide, a similar pattern is observed for nearly all residues in water and in 50% (v/v) TFE, but less marked in water, to indicate much lower populations of folded conformations. In water, the 3−9 (*102*−*108*) region shows poor conformational preference, while the C-terminal 22−26 (*121*−*125*) region exhibits a conformational propensity similar or higher than that observed in 50% TFE.

The NMR conformational shifts confirmed that TFE was not able to induce any significant helical structure in the GH peptide, while micellar SDS is able to stabilize helical segments in the AB peptide. When we compare H^α secondary shifts of regions of the intact protein corresponding to the peptides AB and GH with those obtained for the two peptides in different solvents (Figure 7), it is interesting to note that while peptide AB in 25 mM SDS mimics quite well the behavior of the intact protein in 50% (v/v) TFE, peptide GH shows a definitely less pronounced helicity with respect to the protein. It is worth noting that the inherent conformational flexibility of the AB region of BLG, already highlighted by the H/D exchange experiments (*6*), is reflected by secondary shift values less positive than those of the GH region.

Nativelike Hydrophobic Interactions in Peptide Fragments. Hydrophobic interactions are accepted to be an important driving force in protein folding. Side chains of many residues in short peptides in solution are often quite mobile, and consequently it is difficult to detect NOE cross-peaks involving them. Whenever multiple long-range contacts are observed, especially in TFE which tends to weaken hydrophobic interactions, a strong indication of a potential folding initiation site is provided. Peptide AB only shows (i,i+3) or (i,i+4) NOE contacts consistent with the presence of a α-helix turn. Instead for peptide GH a weak long-range interaction between F6 and L23 could be unambiguously detected in water, while in 50% (v/v) TFE, more side-chain

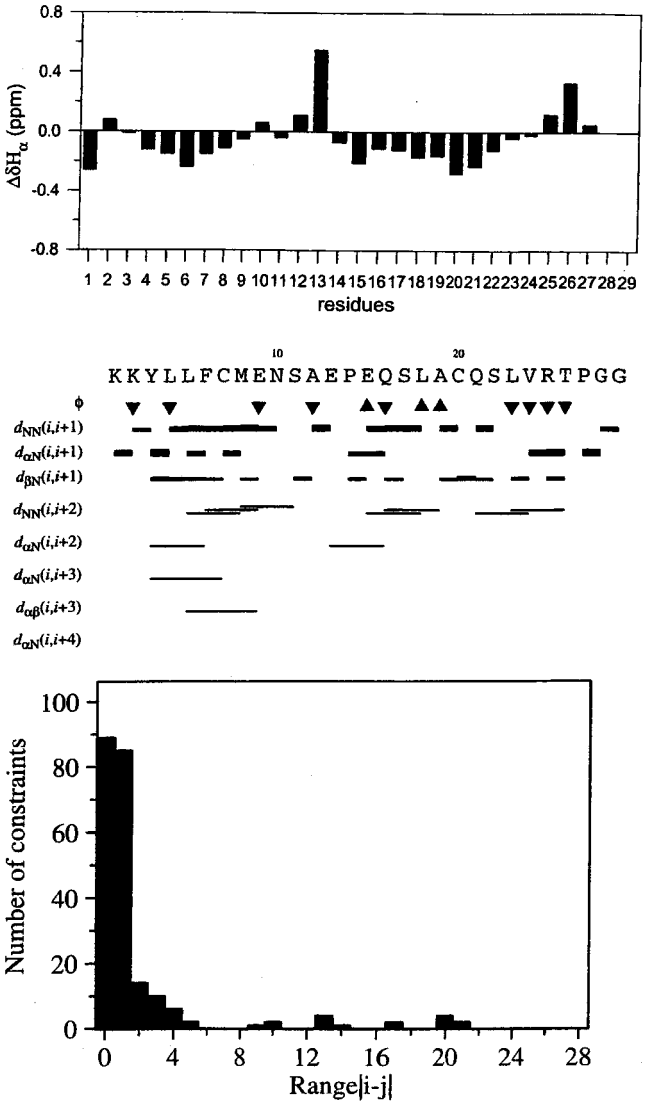

FIGURE 4: GH peptide in 50% (v/v) TFE at 27 °C. Same as for Figure 3.

Table 2: Side-Chain to Side-Chain NOEs Observed for GH Peptide in 50% (v/v) TFE and 27 °C[a]

H_{β^*} K1 (*100*)-$H_{2,6}$ Y3 (*102*)	$H_{3,5}$ F6 (*105*)-H_{γ^*} Q16 (*115*)
H_{δ^*} K1 (*100*)-$H_{3,5}$ Y3 (*102*)	H_4 F6 (*105*)-H_{γ^*} Q16 (*115*)
H_{ϵ^*} K1 (*100*)-H_{β^*} L4 (*103*)	$H_{3,5}$ F6 (*105*)-H_β A19 (*118*)
$H_{2,6}$ Y3 (*102*)-H_{β^*} L4 (*103*)	**$H_{3,5}$ F6 (*105*)-$H_{\delta 1}$ L23 (*122*)**
$H_{3,5}$ Y3 (*102*)-H_{β^*} L4 (*103*)	**$H_{3,5}$ F6 (*105*)-$H_{\delta 2}$ L23 (*122*)**
$H_{2,6}$ Y3 (*102*)-H_{β^*} L5 (*104*)	**H_4 F6 (*105*)-$H_{\delta 1}$ L23 (*122*)**
$H_{2,6}$ Y3 (*102*)-H_{β^*} F6 (*105*)	$H_{\beta 1}$ S11(*110*)-H_{β^*} Q16 (*115*)
$H_{2,6}$ Y3 (*102*)-$H_{\delta 1}$ L23 (*122*)	$H_{\beta 2}$ S11(*110*)-H_{β^*} Q16 (*115*)
$H_{2,6}$ Y3 (*102*)-$H_{\delta 2}$ L23 (*122*)	H_β A12 (*111*)-$H_{\gamma 1}$ E13 (*112*)
$H_{3,5}$ Y3 (*102*)-$H_{\delta 1}$ L23 (*122*)	H_β A12 (*111*)-$H_{\gamma 2}$ E13 (*112*)
$H_{3,5}$ Y3 (*102*)-$H_{\delta 2}$ L23 (*122*)	H_β A12 (*111*)-H_{β^*} Q16 (*115*)
$H_{2,6}$ Y3 (*102*)-$H_{\gamma 1}$ V24 (*123*)	H_β A12 (*111*)-H_{γ^*} Q16 (*115*)
$H_{3,5}$ Y3 (*102*)-H_α V24 (*123*)	H_{β^*} Q16 (*115*)-H_β A19 (*118*)
H_{β^*} L5 (*104*)-$H_{2,6}$ F6 (*105*)	H_{γ^*} Q16 (*115*)-H_β A19 (*118*)
$H_{3,5}$ F6 (*105*)-$H_{\delta 1}$ N10 (*109*)	H_{β^*} Q21 (*120*)-H_{δ^*} R25 (*124*)
$H_{3,5}$ F6 (*105*)-$H_{\delta 2}$ N10 (*109*)	$H_{\beta 1}$ L23 (*122*)-$H_{\gamma 1}$ V24 (*123*)

[a] Numbers in parentheses refer to BLG numbering. NOEs defining the native hydrophobic cluster are reported in bold letters. (∗) Diastereotopic methylenic protons.

to side-chain long-range interactions (i.e., between amino acids separated by more than four residues in the sequence) involving residues Y3, F6, Q16, A19, L23, and V24, were observed (Table 2). The fact that no concentration dependence was observed for the far-UV CD spectra of GH peptide in 50% (v/v) TFE indicated that the peptide is monomeric in these solution conditions and the observed contacts represent intramolecular interactions. Interestingly, the contacts observed in 50% (v/v) TFE, also present in water, between F6 and L23, belonging to G and H strands, respectively, reproduce a native interaction. Indeed the corresponding *F105* and *L122* show a close contact in the

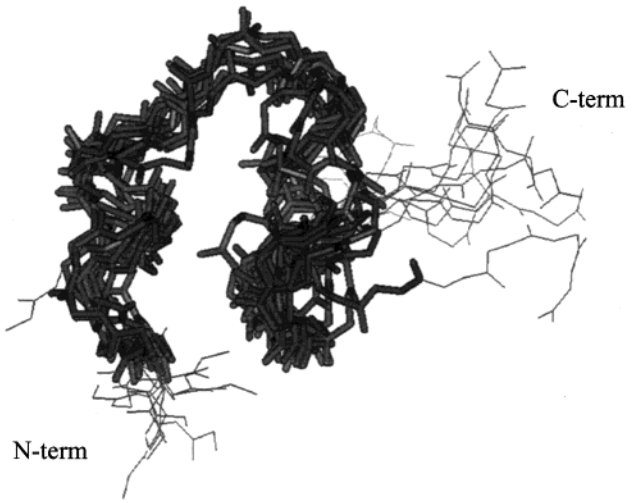

FIGURE 5: Superposition (region 3−25 in bold) of the 10 best energy-minimized DYANA conformers, corresponding to GH peptide in 50% (v/v) TFE solution.

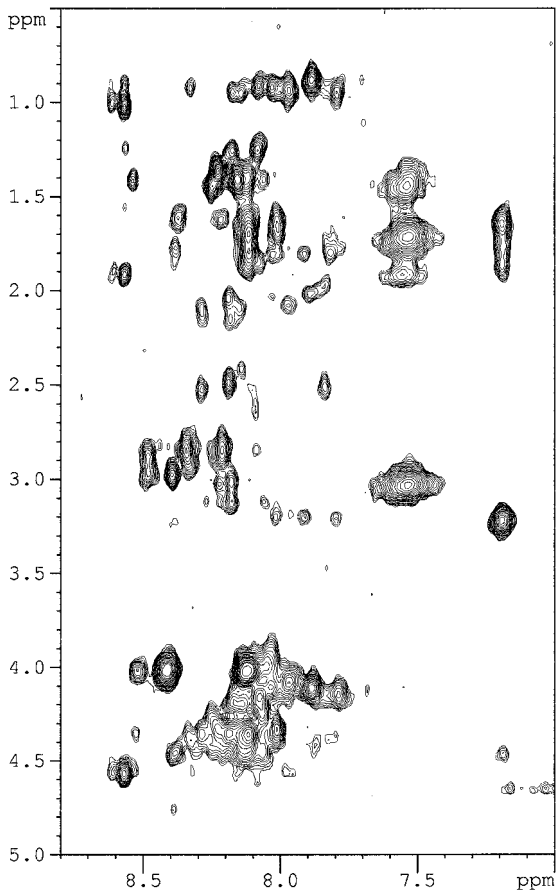

FIGURE 6: Selected region showing the scalar correlations of amides from ^{1}H 500 MHz 2D TOCSY spectrum (mixing time 80 ms) of 1.2 mM EFGH peptide sample in aqueous phosphate buffer solution at pH 2.1 at 37 °C.

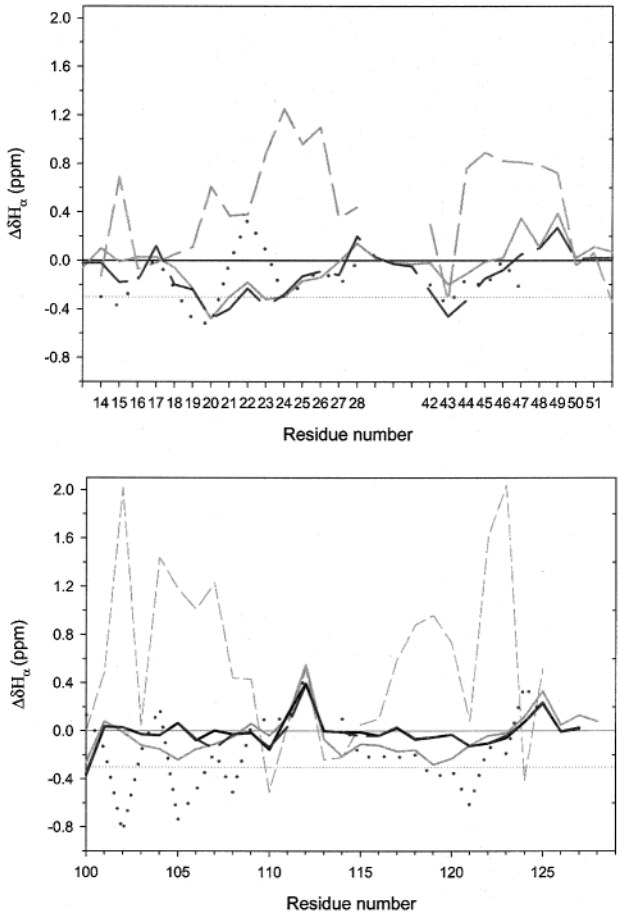

FIGURE 7: Conformational $\Delta\delta$ H^{α} shifts, diagrammatically represented as a function of sequence number (BLG numbering), for AB peptide (top panel) and GH peptide (bottom panel) in different solvents; gray solid line, 50% (v/v) TFE; dark gray medium dash line, 25 mM SDS; black solid line, 2 mM SDS; dark gray short dash line, aqueous phosphate buffer, pH 2.1. For comparison, in each panel, $\Delta\delta$ H^{α} shifts of the corresponding regions of intact BLG in aqueous phosphate buffer at pH 2.1 (grey short dash line) and in 50% (v/v) TFE (dark gray dotted line) are reported.

intact protein and participate to the buried and stable hydrophobic cluster (*2*). The only other residue of the GH interface, belonging to the hydrophobic cluster of BLG, is *L103*. In the GH peptide, the side chain of residue L4 (*L103*) does not show any long-range NOE with the other two side chains while, interestingly, Y3 (*Y102*) shows long-range contacts with F6 and L23, thus playing the role that *L103* has in the native cluster. When the family of structures obtained for peptide GH was analyzed, we actually noticed that the space which was occupied by *L103* in the native hydrophobic cluster, formed with residues *F105* and *L122*, was replaced, in the peptide, by the side chain of Y3 (Figure 8). Y3, F6, and L23 thus reproduce a nativelike cluster (see Discussion). The identification of these native hydrophobic interactions suggests that the GH segment of the protein must have a determinant role in the early events of folding. This suggestion is in line with the observation that the GH interface requires, within the protein, the highest energy to unfold (*6*) and with the recent finding that a nativelike β-hairpin, comprising the GH β-strands, is retained in the cold-denaturated state of BLG (*36*).

Evidence of Residual Structure in the Intact BLG in the Presence of 7 M Urea. Knowledge of the structural properties

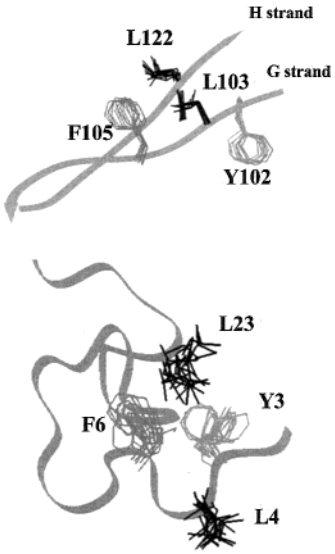

FIGURE 8: Nativelike hydrophobic cluster identified in GH peptide in 50% (v/v) TFE (bottom panel). The superposition of Y3, L4, F6, L23 side chains of the 10 best structures is reported. The superposition of the GH region of BLG (PDB code: 1cj5) (*7*) is reported for comparison (upper panel). The corresponding side chains of *Y102*, *L103*, *F105*, and *L122* are drawn with the same color code.

of the denatured states of proteins is as critical for understanding of protein folding as is knowledge of the native state. The denatured states of many proteins have been shown to contain a significant number of local and long-range interactions (*37*). These persistent structures are considered to be indicative of nucleation sites for the refolding process. In this line, we analyzed the spectra obtained for BLG in the presence of 7 M urea, to check whether we could detect any feature indicative of such residual structure, especially at the level of the GH interface, as suggested by structural data obtained for GH peptide. After treatment with 7 M urea, the protein appeared completely unfolded, as judged from (i) the far and near UV CD spectra typical of random coil polypeptide (*30*), and (ii) 1D and 2D NMR spectra lacking the upfield shifted methyl resonances (*6*). Although structure determination of fully unfolded polypeptides are intrinsically difficult and prohibitive for such a large unlabeled protein, we could, however, perform different types of analysis. We first checked whether any change in the NOE pattern could be detected upon increasing the urea concentration. We have verified that up to 5 M urea, both main-chain to main-chain NOEs, typical of a β structure, and all the side-chain to side-chain NOEs, defining the buried hydrophobic cluster (*2*), which plays an important role in maintaining the stability of the native protein, were conserved. On the basis of the decrease of the normalized intensities of high-field shifted methyl resonances, measured at increasing urea concentrations, a 20−25% folded population is still present at 6 M urea, while at 7 M urea the same peaks are not detected anymore. In 7 M urea, only the NMR spectrum of the unfolded form is seen. The analysis of the 1D ^{1}H aromatic regions of BLG in the presence of variable amounts of urea (0−7 M), indicated that, at 7 M urea, the $H_{2,6}$ and $H_{3,5}$ resonances of *Y102* have not yet reached their random coil value, exhibiting chemical shifts of 7.01 and 6.82 ppm, respectively (see Figure 9). These secondary shifts strongly

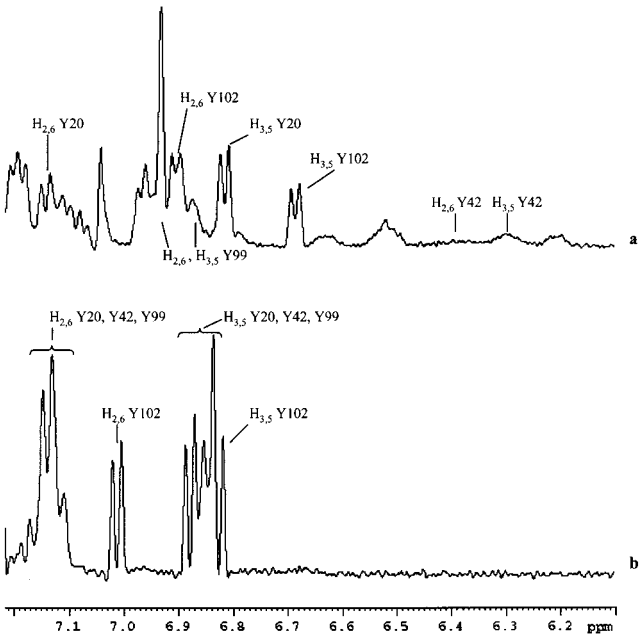

FIGURE 9: Aromatic region of ^{1}H 1D 500 MHz spectra of 1 mM sample of BLG in deuterated phosphate buffer at pH 2.1 and 37 °C in the presence of (a) 0 M urea concentration; (b) 7 M urea concentration. Assignments are reported on the spectra.

evidence that *Y102*, belonging to the GH strand, is involved in the formation of residual structure in the unfolded protein.

DISCUSSION

We have synthesized and characterized a few peptides covering different regions of BLG, which exhibit different stability and folding properties. All of the studied peptides are predominantly unstructured in water, which is not surprising as this tendency has been observed for most short β-sheet-derived peptides studied in aqueous solution. It has been suggested that β-sheet formation, in water at least, may require relatively large peptide fragments. However, we observe here that the EFGH peptide (52 residues), covering four consecutive β-strands, has a strong tendency to aggregate in water, making its NMR structural characterization unfeasible. This behavior implies that EFGH is not an autonomous folding unit and its tendency to aggregate suggests that hydrophobic surfaces are not screened by appropriate structural topology and are exposed, thus decreasing the conformational stability of the peptide. Indeed we have reported on the existence of a surface hydrophobic patch located in a groove between the G, H strands and the terminal helix, characterized by short-range contacts between side chains of residues *A23* (A strand), *Y102*, *L104* (G strands), *F136*, and *A139* (terminal helix), thus indicating the important role played by the terminal helix in stabilizing the EFGH β-core.

The structural tendencies of all synthesized peptides were analyzed in the presence of water and organic solvents, such as TFE and SDS.

Extensive reviews on the possible effect of TFE on protein structure have been reported (*38*, *39*). From all these analyses, the main point which has emerged is that alcohols do not always simulate the protein environment, the effect being dependent on the nature of the amino acid sequences involved and possibly also on the relative importance of tertiary, native, or nonnative hydrophobic interactions between that particular chain segment and the rest of the protein. Only the comparison of the structural preferences observed for peptides covering different regions of the protein with the structure they actually assume in the native protein may clarify the relative role of sequence dependent local and nonlocal interactions. In this respect when we compare the results obtained for AB and GH peptide, we observe that 50% (v/v) TFE does not induce a significant helical population for both peptides, as judged by NMR data. The NMR analysis shows that the two peptides behave differently when SDS is used as cosolvent: GH is essentially random at 2 mM SDS and strongly aggregated at 25 mM SDS, while a helical preference is induced by 25 mM SDS for the AB peptide in the C-terminal region, corresponding to the B strand of the protein. Indeed the solvent accessible B strand, showing, together with strand D, the lowest protection factors (*6*, *8*) and belonging to the most mobile region of the protein, is expected to be mostly influenced by the environment.

The main result of our structural characterization on BLG peptides is the identification of a nativelike hydrophobic cluster in the GH fragment, studied in 50% (v/v) TFE. As already mentioned, it is important to stress here that the presence of the disulfide bridge alone does not warrant for the formation of long-range contacts between Y3, F6, and L23, as shown by the results obtained from molecular dynamics simulations performed in the absence of any NMR restraint except for the disulfide bridge.

When the long-range NOEs observed in 50% (v/v) TFE (reported in Table 2) were compared to those observed in water, the dipolar connectivity $H_{3,5}$F6$-H_{\delta/\delta'}$L23 was the only one which could be unambiguously detected in water. The presence of this NOE supports the hypothesis that a nascent structure in water, presenting nativelike interactions, is stabilized in 50% (v/v) TFE. NOEs among the aromatic side chains of Y3, F6, and the methyl resonances of L23 could not be unambiguously assigned in 2 mM SDS due to severe overlap. We have shown the presence of a residue switch Y3/L4 (*Y102*/*L103*) in the observed hydrophobic cluster of GH peptide in 50% (v/v) TFE: this switch, possibly derived from a rearrangement of the secondary structure, may be guided by the formation of the most stable hydrophobic cluster, in the absence of the tertiary environment. Indeed *Y102* belongs to one of the highest positive surface potential regions of BLG, which has been shown to be largely affected in the computed electrostatic forces by the environmental changes, in good agreement with experimental observations (*4*, *40*). A similar switch of residues has been reported for other proteins, such as, for example, the urea denaturated P434 repressor (*41*) and the mutant F31A of Sso7d protein from *Sulfolobus solfataricus* (*42*). In both cases the formation of the most stable hydrophobic cluster was reported to be the driving force for conformational rearrangement.

Aggregation prevented the complete assignment of EFGH peptide, it is however worth mentioning that long-range NOEs were detected between HN of V47 (*V123*), unambiguously assigned, and $H_{3,5}$ (occurring at 7.12 ppm) of one of the two tyrosines present in the EFGH peptide. It is reasonable to hypothesize, by comparison of the aromatic chemical shifts in EFGH and GH peptides, that the aromatic resonance occurring at 7.12 ppm belongs to Y26 (*Y102*). Other NOEs were also observed between Y26 (*Y102*)

aromatic protons and H_β, H_δ resonances of L46 (*L122*), even though these contacts could not be unambiguously assigned due to overlap. More complete data could not be obtained for EFGH peptide, however, this piece of information contributes to underline the importance of nascent dynamics interactions in this region of the protein, again involving residues *L122* and *Y102*.

At variance with GH region, no long range native interaction was observed in the AB peptide. In this respect, it was recently stressed in the literature the relevance of the relative number of long and short-range contacts in determining the topology of a protein (*43*). When we analyzed the number of long-range interactions (i.e., between amino acids separated by more than four residues) occurring within a couple of strands or between the same couple of strands and the rest of the protein, it appeared that AB peptide showed the highest number of long-range contacts with the rest of the protein and the lowest number of contacts within the AB couple, while GH peptide shows the opposite tendency, thus providing an additional explanation for the different behavior of the two peptides.

All these results find a strong support in two very recent papers (*11*, *36*). In the first, the early folding events of BLG were investigated by ultrarapid mixing techniques in conjunction with hydrogen exchange labeling probed by heteronuclear NMR (*11*). It was shown that, within 2 ms of refolding, well-protected amide protons indicative of a stable hydrogen-bonded structure were found only in a domain comprising β-strands F, G, H, and the main α-helix, thus identifying the folding core of β-lactoglobulin. It was also suggested that the presence of a disulfide bond connecting strands G and H (*C106*−*C119*) and its high content of hydrophobic amino acids give an important contribution to the stability of this domain. The second paper deals with the cold denaturated state of BLG, where a residual structure was observed at the levels of the residues adjacent to the disulfide bond (*C106*−*C119*), suggesting the presence of a nativelike β-hairpin stabilized by the disulfide bond. As reported by Katou et al. (*36*), this β-hairpin, conserved between different conformational states, including the kinetic refolding intermediate, should be of paramount importance for the folding and stability of β-lactoglobulin.

Finally it is worth mentioning that the highest protection factors, measured by burst-phase labeling methods for GH interface, were observed for *M107* and *L122* (*11*). It is interesting to note that the two corresponding residues in GH peptide (M8 and L23) are hydrogen bonded in 15 of the 20 conformers obtained from molecular dynamics simulations. The H-bonds observed in the peptide for the amides of residues M8 and L23 are not typical of a β structure and involve $i+3$ and $i+4$ acceptors, respectively. Large water accessible cavities, as determined by GRASP (*44*), were found in closed proximity to F, G, and H strands (*45*), thus suggesting that in the first steps of BLG refolding, a further rearrangement of the H-bond acceptors may take place through solvent exchange, thus leading to the native H-bond pattern.

ACKNOWLEDGMENT

The authors are indebted to Lucilla Turco and Silvia Romagnoli for technical assistance.

SUPPORTING INFORMATION AVAILABLE

List of proton chemical shifts for AB peptide in 50% (v/v) TFE and 25 mM SDS and for GH peptide in water, 50% (v/v) TFE and 2 mM SDS. This material is available free of charge via the Internet at http://pubs.acs.org.

REFERENCES

1. Hamada, D., Kuroda, Y., Tanaka, T., and Goto, Y. (1995) *J. Mol. Biol. 254* (4), 737−746.
2. Ragona, L., Pusterla, F., Zetta, L., Monaco, H. L., and Molinari, H. (1997) *Folding Des. 2* (5), 281−290.
3. Kuwata, K., Hoshino, M., Era S., Batt, C. A., and Goto, Y. (1998) *J. Mol. Biol. 283* (4), 731−739.
4. Fogolari, F., Ragona, L., Zetta, L., Romagnoli, S., De Kruif, K. G., and Molinari, H. (1998) *FEBS Lett. 436* (2), 149−154.
5. Uhrinova, S., Uhrin, D., Denton, H., Smith, M., Sawyer, L., and Barlow, P. N. (1998) *J. Biomol. NMR 12*, 89−107.
6. Ragona, L., Fogolari, F., Romagnoli, S., Zetta, L., Maubois, J. L., and Molinari, H. (1999) *J. Mol. Biol. 293* (4), 953−969.
7. Kuwata, K., Hoshino, M., Forge, V., Era, S., Batt, C. A., and Goto, Y. (1999) *Protein Sci. 8* (11), 2541−2545.
8. Forge, V., Hoshino, M., Kuwata, K., Arai, M., Kuwajima, K., Batt, C. A., and Goto, Y. (2000) *J. Mol. Biol. 296* (4), 1039−1051.
9. Baldwin, R. L., and Rose, G. D. (1999) *Trends Biochem. Sci. 24*, 77−83.
10. Arai, M., Ikura, T., Semisotnov, G. V., Kihara, H., Amemiya, Y., and Kuwajima, K. (1998) *J. Mol. Biol. 275* (1), 149−162.
11. Kuwata, K., Shastry, R., Cheng, H., Hoshino, M., Batt, C. A., Goto, Y., and Roder, H. (2001) *Nat. Struct. Biol. 8* (2), 151−155.
12. Waltho, J. P., Feher, V. A., Merutka, G., Dyson, H. J., and Wright, P. E. (1993) *Biochemistry 32* (25), 6337−6347.
13. Demarest, S. J., Fairman, R., and Raleigh, D. P. (1998) *J. Mol. Biol. 283*, 279−291.
14. Najbar, L. V., Craik, D. J., Wade, J. D., and McLeish, M. J. (2000) *Biochemistry 39* (19), 5911−5920.
15. Hamada, D., Kuroda, Y., Tanaka, T., and Goto, Y. (1995) *J. Mol. Biol. 254* (4), 737−746.
16. Kuroda, Y., Hamada, D., Tanaka, T., and Goto, Y. (1996) *Folding Des. 1* (4), 255−263.
17. Barlos, K. E., Chatzi, O., Gatos, D., and Stavropulos, G. (1991) *Int. J. Pept. Protein Res. 37*, 513−520.
18. King, D. S., Fields, C. G.; Fields, G. B. (1990) *Int. J. Pept. Protein Res. 42*, 255−266.
19. Ferrer, M., Woodward, C., and Barany, G. (1992) *Int. J. Pept. Protein Res. 40*, 194−207.
20. Chen, Y. H., Yang, J. T., and Chau, K. H. (1974) *Biochemistry, 13*, 3350−3359.
21. Bax, A., and Davis, D. G. (1985) *J. Magn. Reson. 65*, 355−360.
22. Sklenar, V., Piotto, M., Leppik, R., and Saudek, V. (1993) *J. Magn. Reson.* Series A *102*, 241−245.
23. Bartels, C., Xia, T., Billeter, M., Güntert, P., and Wüthrich, K. (1995) *J. Biom. NMR 5*, 1−10.
24. Mumenthaler, C., Güntert P., Braun, W., and Wüthrich, K. (1997) *J. Biomol. NMR 10*, 351−362.
25. Wishart, D. S., Bigam, C. G., Holm, A., Hodges, R. S., and Sykes, B. D. (1995) *J. Biomol. NMR 5*, 67−81.
26. Jiménez, M. A., Nieto, J. L., Herranz, J., Rico, M., and Santoro, J. (1987) *FEBS Lett. 221*, 320−324.
27. Jiménez, M. A., Bruix, M., Gonzalez, C., Blanco, F. J., Nieto, J. L., Herranz, J., and Rico, M. (1993) *Eur. J. Biochem. 211*, 569−581.
28. Güntert, P., Mumenthaler, C., and Wüthrich, K. (1997) *J. Mol. Biol. 273*, 263−296.
29. Kim, Y., and Prestegard, J. H. (1989) *J. Magn. Reson. 84*, 9−13.
30. Ragona, L., Confalonieri, L., Zetta, L., De Kruif, K. G., Mammi, S., Peggion, E., Longhi, R., and Molinari, H. (1999) *Biopolymers 49*, 441−450.

31. Zhong, L., and Johnson, W. C., Jr. (1992) *Proc. Natl. Acad. Sci. 89* (10), 4462−4465.
32. Wu, C. S., Ikeda, K., and Yang, J. T. (1981) *Biochemistry 20* (3), 566−570.
33. Rizo, J., Blanco, F. J., Kobe, B., Bruch, M. D., and Gierasch, L. M. (1993) *Biochemistry 32*, 4881−4894.
34. Munoz, V., Serrano, L., Jimenez, M. A., and Rico, M. (1995) *J. Mol. Biol. 247*, 648−669.
35. Chaffotte, A. F., Guillou, Y., and Goldberg, M. E. (1992) *Biochemistry 31*, 9694−9702.
36. Katou, H., Hoshino, M., Kamikubo, H., Batt, C. A., and Goto, Y. (2001) *J. Mol. Biol. 310*, 471−484.
37. Shortle, D. R. (1996) *Curr. Opin. Struct. Biol. 6*, 24−30.
38. Blanco, F. J., Jimenez, M. A., Pineda, A., Rico, M., Santoro, J., and Nieto, J. L. (1994) *Biochemistry 33*, 6004−6014.
39. Thomas, P. D., and Dill, K. A. (1993) *Protein Sci. 2*, 2050−2065.
40. Fogolari, F., Licciardi, S., Romagnoli, S., Ragona, L., Michelutti, R., Ugolini, R., and Molinari, H., (2000) *Proteins 39*, 317−330.
41. Neri, D., Billeter, M., Wider, G., and Wuthrich, K. (1992) *Science 257*, 1559−1563.
42. Consonni, R., Santomo, L., Fusi, P., Tortora, P., and Zetta, L. (1999) *Biochemistry 38*, 12709−12717.
43. Plaxco, K. W., Simons, K. T., and Baker, D. (1998) *J. Mol. Biol. 277*, 985−994.
44. Nicholls, A., Sharp, K. A., and Honig, B. (1991) *Proteins: Struct., Funct., Genet. 11*, 281−296.
45. Kuwata, K., Li, H., Yamada, H., Batt, C. A., Goto, Y., and Akasaka, K. (2001) *J. Mol. Biol. 305* (5), 1073−1083.

BI011615R